O. J. Botai et al.: Extracting Independent Local Oscillatory Geophysical Signals by Geodetic Tropospheric Delay, IVS 2010 General Meeting Proceedings, p.345–354
http://ivscc.gsfc.nasa.gov/publications/gm2010/botai.pdf

Extracting Independent Local Oscillatory Geophysical Signals by Geodetic Tropospheric Delay

O. J. Botai [1], *L. Combrinck* [2], *V. Sivakumar* [3], *H. Schuh* [4], *J. Böhm* [4]

[1)] *Department of Geography, Geoinformatics and Meteorology, University of Pretoria*
[2)] *Hartebeesthoek Radio Astronomy Observatory*
[3)] *National Laser Center, Council for Scientific and Industrial Research*
[4)] *Institute of Geodesy and Geophysics (IGG), Vienna University of Technology*

Contact author: O. J. Botai, e-mail: joel.botai@up.ac.za

Abstract

Zenith Tropospheric Delay (ZTD) due to water vapor derived from space geodetic techniques and numerical weather prediction simulated-reanalysis data exhibits non-linear and non-stationary properties akin to those in the crucial geophysical signals of interest to the research community. These time series, once decomposed into additive (and stochastic) components, have information about the long term global change (the trend) and other interpretable (quasi-) periodic components such as seasonal cycles and noise. Such stochastic component(s) could be a function that exhibits at most one extremum within a data span or a monotonic function within a certain temporal span. In this contribution, we examine the use of the combined Ensemble Empirical Mode Decomposition (EEMD) and Independent Component Analysis (ICA): the EEMD-ICA algorithm to extract the independent local oscillatory stochastic components in the tropospheric delay derived from the European Centre for Medium-Range Weather Forecasts (ECMWF) over six geodetic sites (HartRAO, Hobart26, Wettzell, Gilcreek, Westford, and Tsukub32). The proposed methodology allows independent geophysical processes to be extracted and assessed. Analysis of the quality index of the Independent Components (ICs) derived for each cluster of local oscillatory components (also called the Intrinsic Mode Functions (IMFs)) for all the geodetic stations considered in the study demonstrate that they are strongly site dependent. Such strong dependency seems to suggest that the localized geophysical signals embedded in the ZTD over the geodetic sites are not correlated. Further, from the viewpoint of non-linear dynamical systems, four geophysical signals—the Quasi-Biennial Oscillation (QBO) index derived from the NCEP/NCAR reanalysis, the Southern Oscillation Index (SOI) anomaly from NCEP, the SIDC monthly Sun Spot Number (SSN), and the Length of Day (LoD)—are linked to the extracted signal components from ZTD. Results from the synchronization analysis show that ZTD and the geophysical signals exhibit (albeit subtle) site dependent phase synchronization index.

1. Introduction

With the increasing ease of collecting and homogenizing tropospheric geodetic data, a long time series of geodetic data sets such as Zenith Tropospheric Delay (ZTD), Water Vapor (WV), and geodetic site coordinates are now available to the scientific community. As a result, the accumulated datasets make it possible to study the geophysical signals embedded in the data. These geophysical signals hold important information about atmosphere–earth system dynamics. However, sequences of these (geodetic) observations have noise, with unknown dependency structure embedded in the data. Until now, the classical techniques of analyzing such series have been subjective and unable to characterize the stochastic structure manifested in the observations. As a result, analyzing such data sets required complex, yet flexible and robust, approaches of objectively manipulating the data.

In non-linear and non-stationary time series, the stochastic global component could be a function which exhibits at most one extremum within a data span or a monotonic function within a certain temporal span (Zhauhua et al., 2007). At first, the mathematical approaches of extracting this component were based on fitting a simple deterministic function (e.g., a linear function) to the data. This method of detrending is clearly suitable for a stationary world and, therefore, may not be robust for real-world applications such as in tropospheric delay due to WV analyses. As the theory of stationary time series developed, the trend was considered as a deterministic component that ought to be removed from the time series in order to make it stationary (Alexandrov et al. 2009). Nevertheless, the deterministic method of trend extraction fails to account for a) the random irregular components, b) the conflicts within the identification of turning points in the trend, and c) the unclear definition of trend, acceptable degree of smoothness, trend-cycles, or long-term structural effects. Some of the prominent approaches of extracting the quasi-period global component in the data include: a) model-based approaches (a stochastic time series model for the data, e.g., ARMA or ARIMA model, are assumed *a priori*); b) nonparametric filtering (which does not require a specification of a model) e.g., the Hodrick-Prescott filter; c) Singular Spectrum Analysis, SSA (a nonparametric methodology that does not require a specification of time series models or a trend *a priori*); d) wavelets; e) Independent Component Analysis (ICA); and f) Empirical Mode Decomposition (EMD). Some of these methods of trend extraction encompass regression analysis or Fourier-based filtering and are based on unjustifiable linearity and stationarity assumptions. Furthermore, the stochastic global component often evolves from the same or part of the same underlying process that generates data, and therefore the temporal structure is often linked to local time scales. As a result, the use of functional forms to represent the unknown embedded trend model could be subjective.

The importance of estimating the slowly evolving changes in tropospheric delay due to WV lies in the role IWV plays in geodetic measurement as well as in climate change. As a result, estimating this stochastic global component is a key element of many studies involving WV variability and its links with the dynamics and precipitation (e.g., Zveryaev and Allan 2005; Trenberth et al. 2005; Schneider et al. 2009). In all these studies, the functional form of the trend is deterministically and subjectively determined. Since the data record under consideration is generated from non-linear and non-stationary underlying processes, a functional form of the trend has to be stochastic and therefore ought not to be pre-selected. Therefore, in order to extract the trend and other (quasi-) periodic components in the data, the process of detrending must be data adaptive (Zhauhua et al. 2007; Alexandrov et al. 2008).

In this study, we examine the use of the combined Independent Component Analysis (ICA) and EMD to extract the local independent components in the tropospheric delay derived from the ECMWF reported by Böhm et al. (2006). Aires et al. (2000) demonstrated a north-south equatorial Atlantic SST linkage by applying the ICA algorithm to study the variability of the tropical sea surface temperature (SST), as well as the links between the variability of ENSO and Atlantic SST. In particular, the Denoising Source Separation (DSS) algorithm (see Särelä and Valpola 2005) can be used to identify hidden geophysical signal components $s_i(t)$ present in the measurements $y_j(t)$ expressed in Equation (1).

$$y_j(t) = \sum_{i=1}^{N} \beta_{i,j} s_i(t) \tag{1}$$

Here, the index j runs over the independent variable measurements, which could be spatial

locations over the discretized observation period t. This generative model describes how the observed data are generated by a process of mixing the underlying signals $s_i(t)$, which are referred to as the ICs. In matrix formulation, the matrix of observations Y, the matrix of the underlying geophysical sources S, the matrix of linear or non-linear combination of the signals or mixing vectors A, and the Gaussian noise δ are mathematically described by a mixing model expressed in Equation (2).

$$Y = AS + \delta \tag{2}$$

Lastly, the causal links between ICs from different IVS and other geophysical records, such as Sun Spot Number (SSN), Length of Day (LoD), Southern Oscillation Index (SOI), and Quasi-Biennial Oscillations (QBO), are examined by use of the angle strength of the phase angle difference between the series, hereafter the mean phase coherence (Mormann et al. 2000). Documenting these results would be useful for understanding the underlying non-stationary and non-linear geophysical signal structure present in the data and for assessing their dependency on each other with applications for the short-term and long-term variability of the atmosphere. An example of research in this direction has been reported by Paluš and Novotná (2009). These contributions would benefit researchers from a diversity of fields.

2. Data and Method

2.1. Data

ZTD over six geodetic IVS sites (see Table 1) spanning 1998 through 2008 were obtained from the Institute of Geodesy and Geophysics (IGG), Technical University of Vienna, Austria (http://www.hg.tuwien.ac.at/∼ecmwf1/VLBI). The ZWD and IWV datasets are derived from ECMWF numerical model simulations (Böhm et al. 2006).

The data under consideration were originally computed at six-hour intervals for the entire temporal span. Monthly values of ZTD were computed for the time span under consideration. The top panel in Figure 1 depicts the apparent seasonality in ZTD (40 cm of ZTD has been added to stations except Hobart26 for better visualization) in all six geodetic IVS stations studied. Geophysical data are significantly affected by seasonal variability. In order to avoid strong seasonality that could mask other important signals (with, e.g., annual, interannual, and interseasonal variability), ZTD data sets were seasonally adjusted by use of the Ratio-to-Moving Average method described by Hanke et al. (2001) and have been plotted in the bottom panel of Figure 1 (here only HartRAO is plotted to illustrate the effect of seasonal adjustment to ZTD). Additionally, we have used monthly time series anomalies of four geophysical signals (here the 1998–2008 time epoch is used): the QBO index derived from the NCEP/NCAR reanalysis; the

Table 1. Geodetic IVS stations used in the study and the number of daily data records for the period 1998 to 2008.

Station	Latitude, Longitude, and Height	# recs
HartRAO	−25.89°, 27.69°, 1416.12 m	4191
Hobart26	−42.80°, 147.44°, 65.53 m	4191
Wettzell	49.15°, 12.88°, 669.56 m	4191
Westford	42.61°, 288.51°, 87.20 m	4191
Tsukub32	36.10°, 140.09°, 85.09 m	4183
Gilcreek	64.98°, 212.50°, 332.52 m	4191

SOI anomaly from NCEP; the SIDC monthly SSN available at www.sidc.oma.be; and the LoD, which is an IERS product.

2.2. Extracting Local Oscillatory Signals in ZTD by Use of EEMD-ICA

The study of ZTD variability is of particular interest, a) because of the inherent mixture of different signal components that exhibit large spatio-temporal time-scales, and b) because the inherent variability is governed by several complex periodic and aperiodic phenomena. In the present study, we propose a combination of Ensemble EMD; hereafter EEMD (see Zhaohua and Huang 2009) and ICA to isolate the low frequency components in ZTD and thereafter investigate the phase dynamics of the oscillating independent components without imposing the assumption of linearity on them. Firstly, the data is decomposed into spectrally independent oscillatory modes called the Intrinsic Mode Functions (IMFs). The resulting IMFs contain inherent additive noise, which dominates the high frequency IMFs. As a result, only those IMFs with lower noise contamination are selected for use in the ICA step. The selection of physically significant IMFs to be used in the ICA stage is a two-step process. In the first step, the IMFs are selected based on the level of noise contamination in the sample. If the IMF_1 is assumed to be highly contaminated, then its amplitude could be used as a reference of the amplitude of the noise contaminated IMFs. Statistically independent IMFs are extracted by selecting only those IMFs whose global energy is at least 30% of the energy of IMF_1. In the second step, ICA reduces the dimensionality of the IMFs adaptively. Given that the number of statistically independent IMFs is smaller than the original IMFs, ICA generally merges the statistically dependent components into the same group and therefore reduces the dimensional space of IMFs.

Furthermore, ICA is a statistical technique that decomposes a series of observations into a linear combination of non-Gaussian random variables that are highly independent components (Hyvärinen 1999). An Extended FastICA (EFICA) algorithm was used to adaptively extract the non-linear components in the data. (FastICA is a Matlab software freely available at http://www.cis.hut.fi/projects/ica/.) The EFICA algorithm utilizes the generalized symmetric FastICA as well as the adaptive selection of the first derivative of the non-linear function called the contrast function (Koldovský et al. 2006) followed by a refinement step. In general, the EEMD-ICA algorithm used in this study can be summarized as follows:

1. Add iid white noise of zero-mean and $\sigma_{iid} = \lambda\sigma_0$ to ZWD. Here, the noise parameter was arbitrarily taken as $\lambda \sim 30\%$.
2. Derive the set of ZTD IMFs by applying EMD until the last IMF is a monotonic function or has at most one extremum.
3. Repeat steps 1 and 2 a number of times, each time using a different randomly generated σ_{iid}. resulting in an ensemble of IMFs (120 ensembles have been used).
4. Average over the ensemble to obtain a set of averaged IMFs.
5. Perform EFICA on the IMFs obtained in step 4 via three steps:
   (a) run the original symmetric FastICA until convergence. In FastICA, the ICs are estimated based on the assumption that the mutually statistically independent components in the mixture exhibit non-Gaussian probability distributions. In order to assess the statistical

independence of the geophysical signals in ZTD, the fourth-order cumulant (kurtosis κ) defined in (3) is used.

$$\kappa(y) = E(y^4) - 3(E(y^2))^2 \tag{3}$$

The kurtosis utilized in computing the statistical independence of the signal present in ZTD could be optimized by using either the fixed-point gradient learning algorithm (Hyvärinen and Oja 1997) or the Newton's method described in Nocedal and Wright (1999).

(b) different non-linearities (the derivative of the score function) are adaptively selected and used to estimate the score functions of the components derived in step (a) above.

(c) components derived from FastICA are fine-tuned using the non-linearities computed in (b) above. This results in an accurate estimation of the unmixing matrix W ($=A^{-1}$).

6. Slowly varying components are selected and multiplied with the mixing matrix to back-reconstruct the selected IMF set.

The causal relationships among the ICs from different stations and between dominant signals of the QBO, SOI, SSN, and LoD are investigated by use of phase synchronization (e.g., Shelter et al. 2007; Kreuz et al. 2007). Synchronization between dynamical systems is an active field of scientific and technical research. For a review and description of the various concepts of synchronization detection, refer to Rosenblum et al. (2001) and Pareda et al. (2005) and others therein.

There are many different approaches of quantifying the degree of synchronization between two systems: linear approaches like the cross correlation or the coherence function, as well as non-linear measures such as mutual information (e.g., Kreuz et al. 2007 and references therein). In the present work, the relation between phases of two geophysical signals and derived tropospheric components over different temporal scales is used as a measure of the presence of interaction between the systems. The relation does not necessarily mean that they are synchronized.

The concept of analytic signal as applied in signal processing is used to define the phase of an arbitrary signal in this work. This analytic signal approach has the advantage that the phase can easily be obtained from scalar time series (Rosenblum and Kurths 1998). For a univariate measurement $x(t)$ the analytic signal $\zeta(t)$ is defined by Equation (4):

$$\zeta(t) = x(t) + j\tilde{x}(t) = A_x^H(t)e^{j\phi_x^H(t)} \tag{4}$$

Here, the function $\tilde{x}$ is the Hilbert transform of $x(t)$ defined by Equation (5);

$$\tilde{x}(t) = \pi^{-1}P\int_{-\infty}^{\infty}\frac{x(\tau)}{t-\tau}d\tau \tag{5}$$

The P in Equation (5) suggests that the integral is taken in the sense of the Cauchy principal value. This implies that the Instantaneous Phases $\phi(t)$ and Instantaneous Amplitude $A(t)$ are uniquely defined from Equation (4). Therefore, given two interacting geophysical signals $x(t)$ and $y(t)$, the phase difference of their analytic signals given by Equation (6) can be used to derive the phase synchronization index defined in Equation (7).

$$\phi_{xy}^H(t) = n\phi_x^H(t) - m\phi_y^H(t) \tag{6}$$

$$\eta = \left| \langle e^{i\phi^H_{xy}(t)} \rangle_t \right| = \sqrt{\langle \cos \phi^H_{xy}(t) \rangle^2_t + \langle \sin \phi^H_{xy}(t) \rangle^2_t} \tag{7}$$

In Equation (6), n and m are integers defining the phase locking ratio (n:m). The synchronization index η ranges from 0 (which suggests that the phase difference is uniformly distributed and there is no phase synchronization) to 1 (which implies that there is perfect synchronization and the phase difference is a constant).

It is worth noting that the use of η to assess the linkage (interaction) between two geophysical signals requires that the independent components in the signal be separated. The rationale behind this analysis is based on the fact that, if the variable represented by one of the series is indeed caused (or at least influenced) by the underlying dynamics in the second series, then the characteristic fluctuations in the ICs derived from the first ICs ought to be preceded by a reaction in the ICs computed from the second series.

3. Results and Discussion

Monthly ZTD delays at the IVS stations (see Table 1) derived from NWP model simulations have been decomposed into the corresponding IMFs. This decomposition stage separates low and high frequency modes. As depicted in Figure 2, the ZTD delay at all the IVS stations (except Tsukub32 which has fewer data records) were decomposed into seven IMFs. We have combined the IMFs with the lowest frequencies (here we have used IMF_6 and IMF_7) in order to generate a weakly oscillating component of the series; hereafter the trend. Figure 2 illustrates a station-dependent trend (this is mode 5 (for Tsukub32) or mode 6 (for all other IVS stations)) with characteristic decadal fluctuations. Additionally, in all the IVS stations, the highly fluctuating IMF (first mode) has oscillating structure with a characteristic period of about one month.

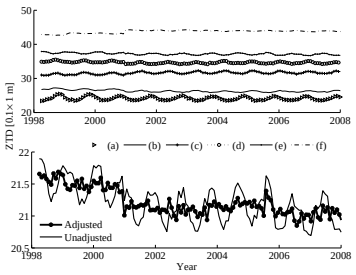

Figure 1. Top panel: tropospheric delay due to water vapor at IVS stations, with 40 mm ZTD added to each station except Hobart26 for better visualization. [**a** → **f**: Tsukub32, Wettzell, Westford, Gilcreek, HartRAO, and Hobart26.] Bottom panel: seasonally adjusted and unadjusted ZTD over HartRAO.

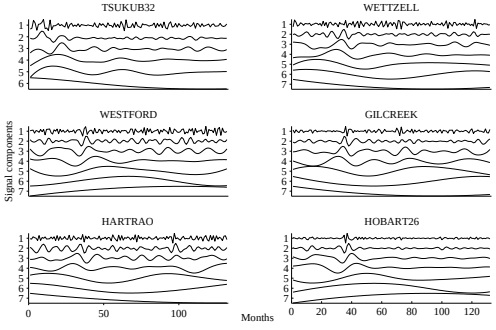

Figure 2. Mode Functions (IMFs) of ZTD series over IVS stations.

Higher periods are not visible because the ZTD series is monthly averaged. The second and third oscillation modes in all the IVS stations exhibit intra-annual and seasonal oscillation periods.

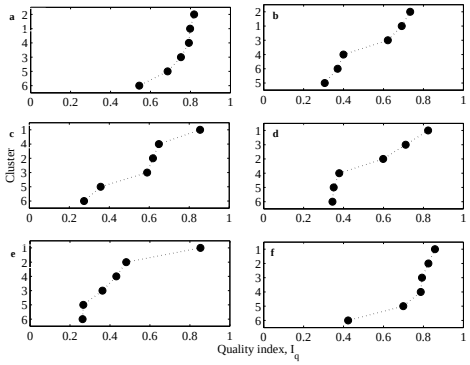

Figure 3. Station dependent quality index Iq of independent components derived from zenith total delay: [**a** → **f**: Tsukub32, Wettzell, Westford, Gilcreek, HartRAO, and Hobart26].

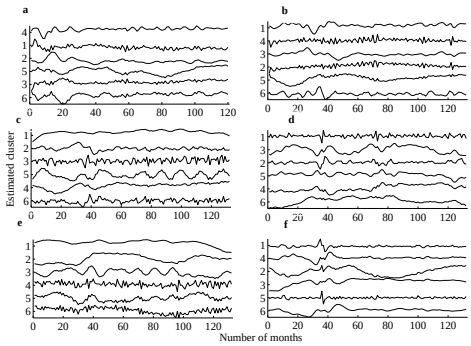

Figure 4. Estimated independent components in zenith total delay: [**a** → **f**: Tsukub32, Wettzell, Westford, Gilcreek, HartRAO, and Hobart26].

These modes could be associated with regional or local weather processes at each IVS site. Annual oscillation periods (corresponding to the fourth and fifth modes) are evident in ZTD series for all IVS stations except Tsukub32. This oscillation pattern could be associated with relatively global geophysical processes such as North Atlantic tele-connection patterns and ENSO.

In the present study, the physical causes of variability of ZTD are assessed by extracting the internal regularities, which include linear or non-linear mixtures of different statistically independent components, by use of ICA. Since we do not have information about the signals embedded in the ZTD data a priori, a blind *source* separation procedure is the natural choice (see for example Särelaä and Valpola 2005). In the FastICA algorithm (Hyvärinen 1999), where a pre-estimate of the unmixing matrix is computed, the statistically independent IMFs are computed based on optimizing contrast functions, i.e., to solve for the signals embedded in the observations; a cost function that either maximizes the non-Gaussianity or minimizes the mutual information is formulated (Del Negro et al. 2008). The quality index I_q of the clusters used to estimate the ICs in the FastICA algorithm are depicted in Figure 3 (here, **a** → **f** corresponds to Tsukub32, Wettzell, Westford, Gilcreek, HartRAO, and Hobart26, respectively). From Figure 3, it can be seen that each of the IVS stations considered in the study contains ICs with unique I_q values. This finding is further evidence that the variability of ZTD at each IVS station is driven primarily by local atmospheric processes.

In all the stations, the magnitude of I_q of all the clusters is generally greater than 0.5. Furthermore, the I_q for all the IVS stations exhibit a knee at cluster 3. This is a strong evidence of some dependence of the geophysical signal derived from ICs at each IVS site as extracted from cluster 3. Therefore, the variability mode of the ZTD could be associated with a geophysical signal with a global geophysical origin such as the climatic tele-connection patterns. Figure 4 depicts the estimated ICs of each cluster (arranged in the order of the clustering quality index) of ZTD at IVS stations. It is evident that the variability structure of the each component is unique at each station. In the present work, the cluster quality index order is used to select the four components that are used to examine the interaction between ZTD and other geophysical signals.

In assessing the nature of linkage between the independent signal components in ZTD with

the geophysical signals, ZTD components that exhibited near Gaussian distribution were selected. Station dependent Gaussian distributed signal components are given in Table 2. Here, a Gaussian shaped distribution depicts a high degree of localization, which suggests that the signal component does not contain spurious components. The linkage between the selected geophysical components (such as those selected in Table 2) is computed and tested by use of the phase synchronization index (see, for instance, Kreuz et al. 2007). In this methodology of non-linear dynamics, the independent components embedded in the mixture of ZWD and other geophysical signals are analyzed focusing on the phases of the fluctuations in each component. From our analysis, it is evident that the signal components extracted from ZTD and the geophysical signals QBO, SOI, SSN, and LoD show some degree of interaction among themselves (see Table 3). As tabulated in Table 3, the phase synchronization index at all IVS stations varies between 0.45 and 0.62 based on the phase locking order 1:1. These values vary across the stations that were considered in this study and, therefore, seem to suggest spatial dependence. As illustrated in Table 3, ZTD observations at Tsukub32 and Westford stations appear not to contain signal components that have dynamical interdependence with QBO, SOI, SSN, and LoD, i.e., the synchronization values are below 0.5.

This signifies weak coupling. The low synchronization index between the ZTD signal components and QBO, SOI, SSN, and LoD could be attributed to strong noise or irregular ZTD fluctuations (which is due to atmospheric dynamics) and non-stationarity (Botai et al. 2009). Further, we observe that Wettzell, Gilcreek, HartRAO, and Hobart exhibit synchronization indices greater than 0.5. The presence of interaction between ZTD measurements and QBO, SOI, SSN, and LoD at the four IVS stations seems to suggest that QBO, SOI, SSN, and LoD signals are indeed embedded in the data.

Table 2. Signal components with approximate Gaussian structure at six IVS stations. Column 2 has selected ZTD components, and column 3 has geophysical signal components.

Station	ZTD	Geophysical
Tsukub32	1, 3, 4	3, 4
Wettzell	1, 2, 3, 4	3, 4
Westford	1, 2, 3	4
Gilcreek	1, 2, 6	3
HartRAO	1, 2	3, 4
Hobart	1, 2, 3	3, 4

Table 3. Synchronization index derived from ZTD and geophysical signals.

VLBI Station	Component pairs	Corresponding phase synchronization index
Wettzell	1-3; 1-4; 2-3; 2-4; 3-3; 3-4; 4-3; 4-4	0.48; 0.58; 0.47; 0.62; 0.43; 0.61; 0.42
Tsukub32	1-3; 1-4; 3-3; 3-4; 4-3; 4-4	0.47; 0.46; 0.47; 0.46; 0.47; 0.45
Westford	1-4; 2-4; 3-4	0.46; 0.49; 0.46
Gilcreek	1-3; 2-3; 6-3	0.55; 0.58; 0.58
HartRAO	1-3; 2-4; 2-3; 2-4	0.54; 0.53; 0.57; 0.50
Hobart	1-3; 1-4; 2-3; 2-4; 3-3; 3-4	0.57; 0.48; 0.57; 0.49; 0.56; 0.48

4. Conclusion

The aim of this study was twofold. Firstly, the combined empirical mode decomposition and independent component analysis methods were used to extract signal components embedded in the tropospheric delay due to water vapor. Results suggest that the tropospheric delay data is a mixture of signal components, each with a different temporal structure. These signal components exhibit spatial dependence suggesting that the high modes of ZTD fluctuations are driven by local atmospheric dynamics. Secondly, in order to assess the linkage of these signal components to geophysical processes, measures of synchronization were done based on the Hilbert transform analytic signal approach. Although further verification on a larger set of IVS stations and other geophysical signals is required, our results reveal that tropospheric delay and the geophysical signals have some dynamical coupling.

References

[1] Aires F., Chédin A., and Nadal J-P., (2000). Independent component analysis of multivariate time series: Application to the tropical SST variability. J. Geophy. Res., 105(13): 17437-17455.

[2] Alexandrov T., (2009). A method of trend extraction using singular spectrum analysis, REVSTAT, 7(1): 1-22.

[3] Boehm J., Werl B., and Schuh H., (2006). Troposphere mapping functions for GPS and very processes in geodetic precipitable water vapor time series, Michael G Sideris (ed). Observing our Changing Earth, International Association of Geodesy Symposia, Springer Berlin Heidelberg, 133: 625-630, doi:. 10.1007/978-3-540-85426-5.

[4] Botai O. J., Combrinck W. L., and deW Rautenbach C. J., (2008). Nonstationary tropospheric long baseline interferometry from European Centre for Medium-Range Weather Forecasts operational analysis data, J. Geophys. Res., 111(B02406): doi:.10.1029.

[5] Darbellay G. A., (1999). An Estimator for Mutual Information based on criterion for independence, Computational statistics and data analysis. 32: 1-17.

[6] Del Negro C., Greco G., Napoli R., and Nunnari G., (2008). Denoising gravity and geomagnetic signals from Etna volcano (Italy) using multivariate methods. Nonlin. Processes Geophy, 15: 735-749.

[7] Hanke J., Wichern D., and Reitsch A., (2001). Business forecasting, Prentice Hall, Upper Saddle River, NJ.

[8] Hyvärinen A., (1999). Fast and Robust Fixed-Point Algorithms for Independent Component Analysis. IEEE Trans. Neutr. Net., 10(3): 626-634.

[9] Hyvärinen A., and Oja E., (1997). A Fast Fixed-Point Algorithm for Independent Component Analysis. Neural computation, 9(7): 1483 - 1492.

[10] Huang N. E., Shen Z., Long S. R., Wu M. C., Shih H. H., Zheng Q., Yen N. .C., Tung C. C. and Liu H. H., (1998). The empirical mode decomposition and the Hilbert spectrum for nonlinear and non-stationary time series analysis. Proc. Roy. Soc. Lond., 454: 903-993.

[11] Koldovský Z., Tichavský P., and Oja E., (2006). Efficient variant of algorithm FastICA for independent component analysis attaining the Cramér-Rao lower bound. IEEE Trans., on Neural Networks, 17 (5): 1265-1277.

[12] Kreuz T., Mormann F., Andrzejak R. G., Kraskov A., Lehnertz K., and Grassberger P., (2007). Measuring synchronisation in coupled model systems: A comparison of different approaches, Physica D 225: 29-42.

[13] Marwan, N., Romano M. C., Thiel M., and Kurths J., (2006). Recurrence plots for the analysis of complex systems, Physics Reports, 438: 237-329.

[14] Mormann F., Lehnertz K., David P., and Elger C. E., (2000). Mean phase coherence as a measure of phase synchronisation and its application to the EEG of epilepsy patients, Physica, D, 144: 358-369.

[15] Nocedal J., and Wright S. J., (1999). Numerical Optimization. Springer-Verlag. ISBN 0-387-98793-2.

[16] Paluš M., and D. Novotná (2009). Phase-coherent oscillatory modes in solar and geomagnetic activity and climate variability, J. Atmos. Sol.-Terr. Phys. 71(8-9), 923-930.

[17] Pareda E., Quiroga R. Q., and Bhattacharya J., (2005). Nonlinear multivariate analysis of neurophysiological signals, Progress in Neurobiology, 77: 1-37.

[18] Rosenblum M., and Kurths J., (1998). Analysing synchronisation phenomena from bivariate data by means of the Hilbert Transform, In: Nonlinear analysis of physiological data, H. Kantz, J. Kurths, and G. Mayer-Kress (eds), Springer, Berlin, 91-99.

[19] Rosenblum M., Pikovsky A., Kurths J., Schafer C., and Tass P. A., (2001). Phase synchronisation: from theory to data analysis, Handbook of biological physics, Elsevier Science, A. J. Hoff (series eds), 4, Neuro-informatics, F. Moss and S. Gielen (eds) Chapter 9, 279-321.

[20] Rybski D., Havlin S., and Bunde A., (2003). Phase synchronization in temperature and precipitation records. Physica A 320, 601-610.

[21] Särelä J., and Valpola H., (2005). Denoising source separation. J. Machine Learning Research, 6: 233-272.

[22] Schelter B., Winterhalder M., Timmer J., and Peifer M., (2007). Testing for phase synchronisation, Physics Letters A, 366: 382-390.

[23] Schneider D.P., Ammann C. M., Otto-Bliesner B. L., and Kaufman D. S., (2009). Climate response to large, high latitude and low-latitude volcanic eruptions in the Community Climate System Model, J. Geophys. Res. Atmosph., 104 (D15101): doi:. 10.1029/2008JD011222.

[24] Shannon C. E., and Weaver W., (1949). The mathematical theory of communication. University of Illinois press.

[25] Trenberth K. E., Fasullo J., and Smith L., (2005). Trends and variability in column-integrated water vapour. Clim. Dyn., 24: 741-758, doi:, 10.1007/s00382-005-0017-4.

[26] Zhaohua W. and N. E. Huang, (2009). Ensemble empirical mode decomposition: a noise-assisted data analysis method, Advances in Data Adaptive Analysis, 1(1): 1-41.

[27] Zhauhua W., Huang N. E., Long S. R., and Peng C..K., (2007). On the trend, detrending and variability of nonlinear and nonstationary time series, PNAS, 104(38): 14889-14894.